

Synthesis and Antitrypanosomal and Mechanistic Studies of a Series of 2-Arylquinazolin-4-hydrazines: A Hydrazine Moiety as a Selective, Safe, and Specific Pharmacophore to Design Antitrypanosomal Agents Targeting NO Release

Angel H. Romero,* Elena Aguilera, Lourdes Gotopo, Jaime Charris, Noris Rodríguez, Henry Oviedo, Belén Dávila, Gustavo Cabrera, and Hugo Cerecetto*



Cite This: <https://doi.org/10.1021/acsomega.2c06455>



Read Online

ACCESS |



Metrics & More

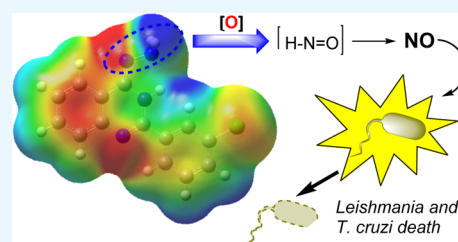


Article Recommendations



Supporting Information

ABSTRACT: Nitric oxide (NO) represents a valuable target to design antitrypanosomal agents by its high toxicity against trypanosomatids and minimal side effects on host macrophages. The progress of NO-donors as antitrypanosomal has been restricted by the high toxicity of their agents, which usually is based on NO-heterocycles and metallic NO-complexes. Herein, we carried out the design of a new class of NO-donors based on the susceptibility of the hydrazine moiety connected to an electron-deficient ring to be reduced to the amine moiety with release of NO. Then, a series of novel 2-arylquinazolin-4-hydrazine, with the potential ability to disrupt the parasite folate metabolism, were synthesized. Their *in vitro* evaluation against *Leishmania* and *Trypanosoma cruzi* parasites and mechanistic aspects were investigated. The compounds displayed significant leishmanicidal activity, identifying three potential candidates, that is, **3b**, **3c**, and **3f**, for further assays by their good anti-mastigote activities against *Leishmania braziliensis*, low toxicity, non-mutagenicity, and good ADME profile. Against *T. cruzi* parasites, derivatives **3b**, **3c**, and **3e** displayed interesting levels of activities and selectivities. Mechanistic studies revealed that the 2-arylquinazolin-4-hydrazines act as either antifolate or NO-donor agents. NMR, fluorescence, and theoretical studies supported the fact that the quinazolin-hydrazine decomposed easily in an oxidative environment via cleavage of the N–N bond to release the corresponding heterocyclic-amine and NO. Generation of NO from axenic parasites was confirmed by the Griess test. All the evidence showed the potential of hydrazine connected to the electron-deficient ring to design effective and safe NO-donors against trypanosomatids.



INTRODUCTION

Neglected tropical diseases (NTDs) such as leishmaniasis and Chagas disease are caused by obligate intracellular parasites of *Leishmania* spp. and *Trypanosoma cruzi*, respectively, which are transmitted to humans by insects.¹ Chagas disease is located in 21 countries of Latin America with approximately 6–7 million infected and more than 70 million people at risk,² whereas the leishmaniasis is prevalent in 88 countries worldwide with 350 million people at risk of acquiring the disease.³

At the moment, treatments against these NTDs are severely limited and only a few approved drugs are present: (i) benznidazol and nifurtimox against Chagas disease and (ii) pentavalent antimonials (e.g., glucantime and pentostam) against Leishmaniasis. A second line of anti-Chagas drugs such as antifungal azoles (e.g., osaconazole, ketoconazole, ravuconazole, etc.) and leishmanicidal agents including pentamidine, amphotericin B, and miltefosine are frequently used when the first line failed.⁴ However, these drugs present several disadvantages including high toxicity (affecting the heart, liver, and kidneys), mutagenicity, high costs, low efficiency, and complex administration protocols.⁴ As a

consequence of the emergent parasite resistance, toxicity issues, and the lack of efficacy of these types of clinical agents against NTDs, new effective and safer drugs are urgently needed to open new lights toward the solution of these public health problems. Designing a specific and selective anti-trypanosomal agent is essential to know about the pivotal aspect in the survival of parasites. It is well documented that NO is a molecule considerably toxic for trypanosomatids and its production, for example, by infected macrophages as an immunological response, affects the cell proliferation of *T. cruzi* and *Leishmania* parasites into mammal cells.^{5–7} Then, the *in situ* release of NO via drug decomposition or via immunologic activation represents an attractive strategy to design selective antitrypanosomal agents. Nowadays, there are a few examples

Received: October 6, 2022

Accepted: November 23, 2022

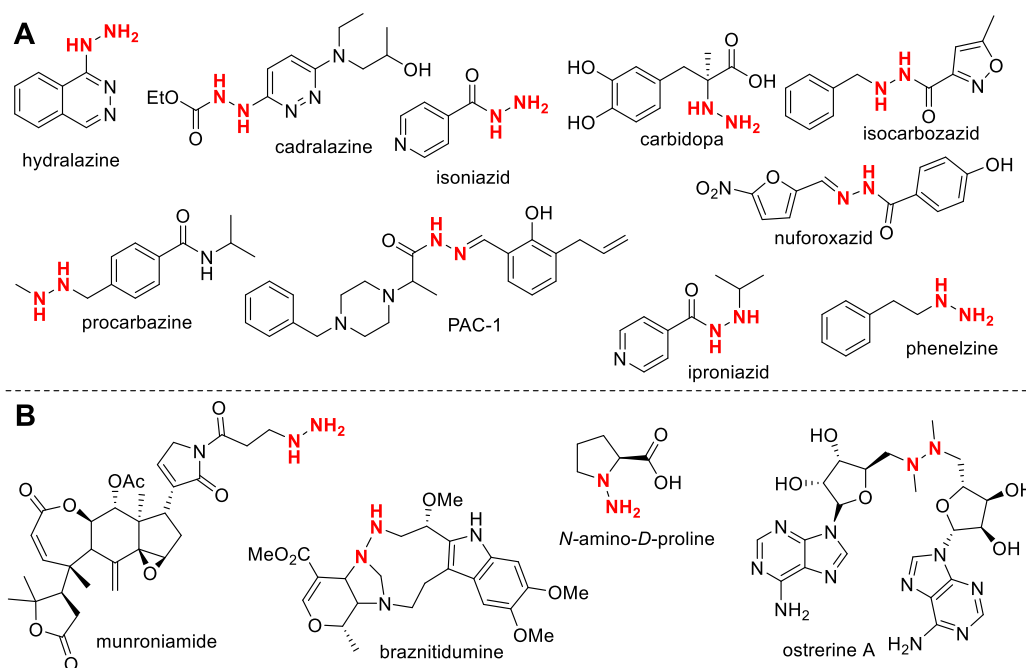
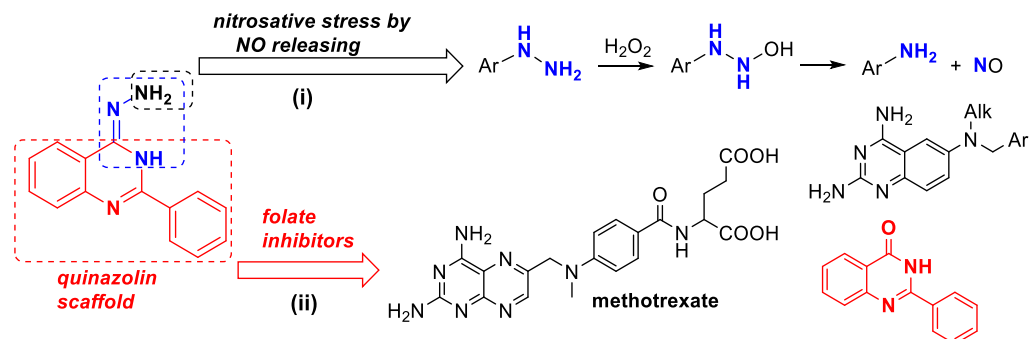


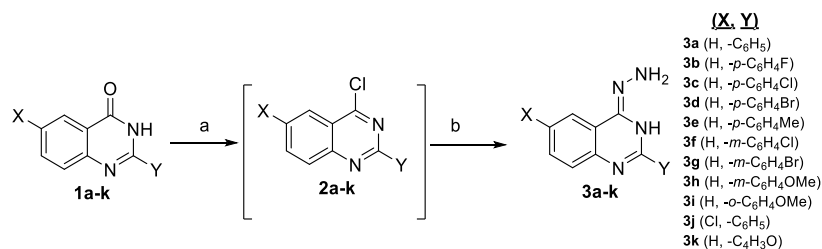
Figure 1. Hydrazines/hydrazides containing therapeutic agents (A) and natural products (B).

Chart 1. Principle Design of 2-Arylquinazolin-4-hydrazines Targeting Dual Action: (i) NO-Donor and (ii) Folate Inhibitor.



60 of antitrypanosomal agents targeting NO production.⁷ Most of
 61 them are represented by metallic complexes containing the
 62 NO-ligand, which release NO through cleavage from the
 63 metal–NO bond.^{8–12} Other examples consisted of organic
 64 NO-donor heterocycles, which are able to release NO via ring
 65 opening of the hetero-ring-masked NO-releasing moiety.^{13–15}
 66 Despite good antitrypanosomal activity of compounds based
 67 on two mentioned chemical systems, the low selectivity with
 68 toxicity consequences is the main limitation of the NO-donors,
 69 in which the design of the new chemical form to access the NO
 70 in situ without side effects on host cells is important.
 71 In this sense, the hydrazine (–NH₂–NH₂–) function
 72 represents an attractive moiety to design NO-donors because
 73 of the fact that the chemical functionality has shown to be
 74 highly sensitive to decompose via the oxidative process under
 75 basic or neutral conditions with generation of NO. For
 76 example, Rehse and Shahrouri showed the ability of a
 77 hydrazine moiety connected to an electron-deficient aromatic
 78 ring (e.g., phthalazine) to induce the release of NO in solution
 79 upon oxidative conditions, which was attributed to a plausible
 80 oxidative decomposition of the hydrazine moiety.¹⁶ Other
 81 examples have shown the susceptibility of the hydrazine moiety
 82 to decompose in the presence of catalytic transition metals at

room temperature.^{17–19} Nevertheless, the use of hydrazine as a
 83 pharmacophore represents a controversial topic within
 84 medicinal chemistry because it is considered a promiscuous
 85 group.²⁰ In our favor, we can mention that there are a large
 86 number of approved drugs containing the hydrazine moiety
 87 with clinical uses including hydralazine and cadralazine as anti-
 88 hypertensives, isoniazid, isocarboxazid, and nifuroxazid as
 89 antibiotics, procarbazine as antineoplastic, phenelzine and
 90 iproniazid as antidepressants, and carbidopa as the anti-
 91 Parkinson drug (Figure 1A).^{21,22} Also, the hydrazine can be
 92 found in natural products with biological activity.^{23,24} Sperry
 93 and Blair showed that over 200 natural products contain the
 94 N–N bond motif, although only four of them presented the
 95 simple hydrazine moiety, including N-amino-D-proline,
 96 munroniamide, braznitidimine, and ostarine A (Figure 1B).
 97 Recently, the incorporation of the hydrazine moiety has
 98 received great attention for the development of active
 99 compounds against diverse types of pathologies.^{25–29} Regarding
 100 the use of hydrazine to design leishmanicidal agents,
 101 aminoquinoline derivatives hybridized with the isoniazid or
 102 hydrazine group have promoted a good leishmanicidal activity
 103 against intracellular amastigotes of *Leishmania braziliensis*
 104 without an apparent cytotoxic effect.^{15,30,31}

Scheme 1. Synthesis of 2-Arylquinazolin-4-hydrazine 3a–k^a

^aConditions: (a) 2-arylquinazolin-4(3H)-ones **1a–k**, POCl₃ (6 equiv), 100 °C, 4–5 h and (b) compound **2a–k**, NH₂–NH₂·xH₂O (4 equiv), ethanol, 70 °C, 2 h.

Table 1. In Vitro Growth Inhibitory Effects of the Compounds 3a–k and 4a–c and References Against *Leishmania* and *T. cruzi*

compounds	promastigote, IC ₅₀ (μM) (PGI) ^a		epimastigote, IC ₅₀ (μM) (PGI) ^a	
	<i>L. braziliensis</i>	<i>L. infantum</i>	<i>T. cruzi</i>	
1	3a	4.53 ± 0.23	12.67 ± 0.74	>25.00 (42.7)
2	3b	3.85 ± 0.17	5.01 ± 0.31	17.95 ± 1.21
3	3c	5.12 ± 0.32	1.56 ± 0.09	11.48 ± 0.49
4	3d	6.20 ± 0.38	2.13 ± 0.12	14.32 ± 0.87
5	3e	10.06 ± 0.48	1.20 ± 0.08	17.99 ± 1.11
6	3f	5.63 ± 0.36	4.55 ± 0.29	>25.00 (38.0)
7	3g	>25.0 (27.3) ^a	21.14 ± 1.21	>25.00 (21.4)
8	3h	12.21 ± 0.76	>25.0 (47.2)	>25.00 (10.1)
9	3i	>25.0 (49.23) ^a	>25.0 (28.3)	>25.00 (11.9)
10	3j	>25.0 (43.23) ^a	19.67 ± 1.78	>25.00 (37.7)
11	3k	>25.0 (46.56) ^a	14.03 ± 0.91	>25.00 (8.56)
12	4a	>25.0 (20.12) ^a	>25.0 (18.56)	>25.0 (10.22)
13	4b	>25.0 (18.56) ^a	>25.0 (12.34)	>25.0 (9.66)
14	4c	>25.0 (12.45) ^a	>25.0 (9.45)	>25.0 (6.54)
15	miltefosine ^b	8.78 ± 0.41	10.60 ± 0.46	N.D.
16	glucantime ^b	32.00 ± 1.78	N.D.	N.D.
17	nifurtimox ^c	N.D.	N.D.	7.7 ± 0.5

^aPGI: percentage growth inhibition of the parasite cell, determined at 25 μM. ^bLeishmanicidal reference. ^cAnti-Chagasic ref 36. Note: parameters marked in bold indicate a pronounced antiparasite activity. N.D.: not determined.

106 With all these arguments, herein we designed a series of new
 107 2-arylquinazolin-4-hydrazine derivatives, where the hydrazine
 108 moiety is connected to an electron-deficient heterocycle, the 2-
 109 arylquinazoline, with a demonstrated anti-trypanosomatid
 110 activity against *Leishmania* parasites.³²

111 ■ RESULTS AND DISCUSSION

112 **Design and Synthesis.** The design of the target 2-
 113 arylquinazolin-4-hydrazines **3a–k** was inspired by a series of
 114 active 2-arylquinazolin-4(3H)-ones, which showed remarkable
 115 leishmanicidal activity against *Leishmania* parasites with the
 116 ability to interfere with the parasite folate metabolism.³²
 117 Herein, we replaced the oxygen atom by a hydrazine moiety at
 118 4-position of the 2-arylquinazoline core to generate a dual-
 119 targeting system: (i) NO released by the in situ oxidation of
 120 the hydrazine moiety placed in the electron-deficient quinazo-
 121 line ring and (ii) the antifolate pathway by the 2-arylquinazo-
 122 line core (Chart 1). The selection of functionalities for the
 123 designed 2-arylquinazolines **3a–k** (Scheme 1) was focused on
 124 those aryl functionalities that led to the best activity/toxicity

profile in the 2-arylquinazolin-4(3H)-ones: 4-Cl-, 3-OMe-, and
 4-F-phenyl.³² Other 3-chlorophenyl (**3f**) or 3-bromophenyl
 (3g) electron-deficient aryl functionalities also were considered
 in order to construct compounds consisting of an electron-
 deficient ring connected to a hydrazine group, which is
 convenient for the decomposition of the hydrazine moiety.
 16–19 Also, we prepared a 6-chloro-substituted derivative
 (3j), but the scaffold did not explode by its low solubility.^{32,33}

The preparation of 2-arylquinazolin-4-hydrazines **3a–k** was
 performed from their corresponding 2-arylquinazolin-4(3H)-
 ones **1a–k**³³ through a sequential two-step reaction (Scheme
 1).^{34,35} First, **1a–k** were reacted with phosphorus oxychloride
 to give the corresponding 2-aryl-4-chloroquinazolines **2a–k**,
 which were sufficiently pure for the next reaction step. They
 were reacted with hydrazine in ethanol to give the desired 2-
 arylquinazolin-4-hydrazine **3a–k** in excellent yields (83–91%).
 A second group of heterocycle hydrazines based on
 phthalazines **4a**, **4b**, and **4c** (Table 1) were prepared previously
 from phthalazin-1,4-dione^{34,35} to complement our structural
 comparisons. Experimental details and spectroscopic informa-

Table 2. Cytotoxicity, *Leishmania* Antiamastigote Activity, and Selectivity Indexes of Active Derivatives 3a–f

compounds	peritoneal macrophage, CC ₅₀ (μM)	J774.1A macrophage, CC ₅₀ (μM)	amastigote, IC ₅₀ (μM) <i>L. braziliensis</i> (S.I. _{Leishmania}) ^a	epimastigote, IC ₅₀ (μM) <i>T. cruzi</i> (S.I. _{T.cruzi}) ^b
1 3a	61.02 ± 2.34	90.20 ± 4.32	8.26 ± 0.45 (7.4)	<3.6
2 3b	>100.0	>120.00	7.41 ± 0.39 (>13.5)	>6.7
3 3c	89.86 ± 3.77	104.78 ± 5.66	8.96 ± 0.53 (10.0)	9.1
4 3d	77.98 ± 3.89	78.59 ± 3.99	12.67 ± 0.78 (6.2)	5.5
5 3e	84.76 ± 3.67	114.58 ± 5.43	13.99 ± 0.89 (6.1)	6.4
6 3f	>100.0	>120.0	8.43 ± 0.51 (>11.9)	no active
7 miltefosine	67.78 ± 3.11	72.34 ± 3.45	21.23 ± 1.13 (3.2)	
8 glucantime	138.22 ± 10.11		12.21 ± 2.12 (11.3)	
9 nifurtimox		280.0 ± 4.00 ^c		36 ^c

^aSelectivity indexes calculated from ratio between the CC₅₀ (peritoneal macrophage) and IC₅₀ (amastigotes of *L. braziliensis*). ^bSelectivity indexes calculated from the ratio between the CC₅₀ (J774.1A) and IC₅₀ of epimastigotes (*T. cruzi*). ^cFrom ref 36.

tion for pure compounds can be found in the Supporting Information. A comparative analysis based on NMR spectra and theoretical calculations revealed that the compound is under the tautomeric form: (Z)-1-(2-phenylquinazolin-4(3H)-ylidene)hydrazine. A detailed discussion can be found in Section S2 of the Supporting Information. Table S1 shows clearly that the imine-tautomer is energetically more accessible than the hydrazine-tautomer.

Biological Evaluation. All synthesized compounds were initially tested against promastigotes of *L. braziliensis* and *L. infantum* and against epimastigotes of *T. cruzi* (Table 1). In general, the compound showed a higher activity against *Leishmania* than against *T. cruzi*. Against *Leishmania*, it should be noted that some 2-arylquinazolin-4-hydrazines exhibited a higher activity against than miltefosine and glucantime references. In general, compounds were barely more active against *L. infantum* parasite than against *L. braziliensis*. Six of them (3a, 3b, 3c, 3d, 3e, and 3f) displayed low-micromolar IC₅₀ values ranging from 3.85 to 10.06 μM and from 1.20 to 12.67 μM against *L. braziliensis* and *L. infantum*, respectively. Curiously, the derivative 3e showed the highest activity against promastigotes of *L. infantum* with an IC₅₀ value of 1.2 μM and a discrete activity against *L. braziliensis* (IC₅₀ = 10.06 μM). In contrast, compound 3h was active against *L. braziliensis* (12.21 μM) but inactive against *L. infantum*. Meanwhile, the quinazolines 3g (3-Br-phenyl) and 3j (X, Y = Cl) displayed discrete responses against both *Leishmania* strains, whereas 3i did not show activity. The latter may be mainly attributed to its poor solubilities. Interestingly, the active compounds 3c, 3d, and 3e were significantly more active than their corresponding 2-arylquinazolin-4(3H)-one parent compounds against promastigote *Leishmania* parasites,³² which puts in evidence that the incorporation of the hydrazine moiety enhances the potency of the 2-arylquinazoline as leishmanicidal.

Regarding *T. cruzi* activity, derivatives 3b, 3c, 3d, and 3e showed the best anti-epimastigote activities with IC₅₀ values of 17.95, 11.48, 14.32, and 17.99 μM, respectively. Similar to antileishmanial response, compounds 3g to 3j demonstrated modest responses against *T. cruzi*. The active compounds against *Leishmania*, 3a and 3f, showed weak anti-*T. cruzi* activities with PGI values of 42.7 and 38% at 25 μM, respectively. The rest of the derivatives displayed PGI magnitudes less than 22% at 25 μM, except 3j (PGI = 37.7%). The 2-arylquinazolin-4-hydrazines were less active than nifurtimox by two- to threefold. As an anti-*T. cruzi* agent, it should be noted that 2-arylquinazolin-4-hydrazines bearing electron-withdrawing moieties at 4-position of the aryl ring

(e.g., 4F, 4Cl, and 4Br) were the most active compounds. Compound 3e (4-Me-phenyl) exhibited an activity comparable to electron-deficient derivatives 3c and 3d. Compounds 3h and 3i were also poorly active. On the other hand, against both parasites, the phthalazin-hydrazine, 4a, 4b, and 4c, they did not show antitrypanosomal activities (PGI < 20%). It reflects the fact that the 2-arylquinazoline was a more convenient scaffold than phthalazine to design hydrazine derivatives, and the incorporation of the electron-withdrawing aryl moiety is preferred to generate active antitrypanosomal agents.

Next, the most active compounds (3a–3f) were selected for cytotoxic evaluation using (i) primary peritoneal macrophages^{32,35} and (ii) J774.1A macrophages³⁶ (Table 2). The 2-arylquinazolin-4-hydrazines 3b and 3f were identified as the least toxic compounds with CC₅₀ values higher than 100 μM against both macrophage lines. Derivatives 3c and 3e displayed CC₅₀ of 104.78 and 114.58 μM against J774.1A macrophages, respectively, and CC₅₀ values of 89.86 and 84.76 μM against peritoneal macrophages, respectively. Meanwhile, compounds 3a and 3d were recognized as the most toxic agents among the studied active 2-arylquinazolin-4-hydrazines, CC₅₀ values ranging from 60 to 90 μM.

Then, we evaluated the potential of these six compounds against infective intracellular amastigotes of *L. braziliensis*.³² Compounds 3a, 3b, 3c, and 3f showed the best antiamastigote activity having IC₅₀ values between 7.41 and 8.96 μM against *L. braziliensis*, whereas compounds 3d and 3e displayed good IC₅₀, 12.67 and 13.99 μM, respectively. The antiamastigote activity of the compounds 3b, 3c and 3f were barely higher than that found for glucantime reference (IC₅₀ = 12.21 μM). Then, selectivity index (S.I.) values relative to *Leishmania* were calculated as the ratio of the CC₅₀ value of the macrophage (peritoneal) to IC₅₀ of amastigotes of *L. braziliensis*. Derivatives 3b, 3c, and 3f showed the best S.I., with values higher than 10, which is in the same range compared to glucantime and better than miltefosine S.I. All six derivatives displayed higher antiamastigote activity and selectivity than miltefosine. The rest of the compounds, 3a, 3d, and 3e, showed S.I. values between 6.1 and 7.5. On the other hand, as an anti-*T. cruzi* agent, the compounds 3b–3e showed S.I. values higher than 5.5 (Table 2). Compound 3a displayed an S.I. lower than 3.6, with nifurtimox (S.I. = 36) being more selective than quinazolin-hydrazines.³⁶

Drug-like Profiles. First, drug-like properties for active compounds 3b, 3c, and 3f were studied in silico using the Swiss-ADME platform.³⁷ Physicochemical properties (lipophilicity, water solubility, pharmacokinetic properties, and

Table 3. In Silico Physicochemical, Pharmacokinetic, and Drug-likeness Parameters of 3b, 3c, and 3f

type of parameter	parameter	3b	3c and 3f
physicochemical properties	M.W. (g/mol) ^a	254.26	270.72
	N ^o rotatable bonds	2	2
	N ^o H-bond acceptors	4	3
	N ^o H-bond donors	2	2
	molar refractivity	72.14	77.19
	TPSA (Å ²) ^b	63.83	63.83
lipophilicity	log P _{o/w} (iLOGP)	2.35	2.07
	log P _{o/w} (XLOGP3)	3.18	3.71
	log P _{o/w} (WLOGP)	2.95	3.05
	log P _{o/w} (MLOGP)	3.19	3.31
	log P _{o/w} (SILICOS-IT)	2.33	2.55
	consensus log P _{o/w}	2.80	2.94
water solubility	log S (ESOL)	−3.91	−4.35
	solubility	123 μM (soluble)	45 μM (moderately soluble)
	log S (Ali)	−4.19	−4.74
	solubility	64.3 μM (moderately soluble)	18.1 μM (moderately soluble)
pharmacokinetic properties	GI absorption ^c	high	high
	BBB permeant ^d	yes	yes
	P-gp substrate ^e	no	no
	CYP1A2 inhibitor	yes	yes
	CYP2C19 inhibitor	yes	yes
	CYP2C9 inhibitor	no	no
	CYP2D6 inhibitor	no	no
	CYP3A4 inhibitor	no	no
	log K _p (skin permeation)	−5.59 cm/s	−5.32 cm/s
drug-likeness	Lipinski	fit; 0 violation	fit; 0 violation
	Ghose	fit	fit
	Veber	fit	fit
	Egan	fit	fit
	Muegge	fit	fit
	bioavailability score	0.55	0.55
	medicinal chemistry	PAINS	0 alert
	Brenk	1 alerts: hydrazine	1 alert: hydrazine
	lead-likeness	fit	do not fit; 1 violation: XLOGP3 > 3.5

^aMW: molecular weight. ^bTPSA: topological polar surface area. ^cG.I.: gastrointestinal. ^dBBB: blood–brain barrier. ^eP-gp: P-glycoprotein. Drug-likeness maps are found in Figure S3.

239 other drug-likeness predictors) are summarized in Table 3. In
 240 general, the compounds showed good physicochemical
 241 properties within Lipinski,³⁸ Ghose, Veber, Egan, and Muegge
 242 rules.³⁹ Meanwhile, the compounds displayed a good aqueous
 243 solubility (from 43 to 125 μM), which is in good concordance
 244 with the appreciable solubility of the compounds 3b, 3c, and 3f
 245 in culture. Within the pharmacokinetic properties, compounds
 246 showed high G.I. (gastro-intestinal) indexes, positive BBB
 247 (blood brain barrier) permeabilities, good skin permeation
 248 (Log K_p by about −5.3/−5.6 cm/s), and a negative substrate
 249 for P-gp. Compounds showed to be potential substrates for
 250 CYP1A2 and CYP2C19 proteins but not for the CYP2C9,
 251 CYP2D6, and CYP3A4 proteins. Within medicinal chemistry,
 252 no PAINS moieties were identified from the 2-arylquinazolin-
 253 4-hydrazine, and only an alert was indicated for the hydrazine.
 254 To support this, we passed the three compounds through a
 255 filter for recognizing PAINS,⁴⁰ and none of them represent a
 256 PAINS. Finally, to evaluate the security of the compounds, we
 257 performed the Ames test to discard the mutagenic effect
 258 derived from the interaction of compounds with biological
 259 systems. The mutagenic assay was performed using a
 260 genetically modified *Salmonella Typhimurium* TA 98 for the
 261 compound 3c.⁴¹ From the Ames test, compound 3c was

262 identified as a non-mutagenic agent due to the fact that it was
 263 not able to at least double the number of colonies of
 264 spontaneous revertant colonies (0.0 μg/plate of compound)
 265 for at least two consecutive dose levels,⁴¹ while revertant
 266 colonies were obtained with the mutagenic 4-nitro-*o*-phenyl-
 267 enediamine (NPD) positive control (Table 4). Thus, the
 268 hydrazine connected to 2-arylquinazolin at 4-position emerges
 269 as a safe pharmacophore from the toxic and mutagenic point of
 270 view.

Mechanism of Action Studies. Herein, we focused on
 271 validating (i) antifolate activity and (ii) NO production via
 272

Table 4. Ames Results in TA 98 Strain

comp.	doses (μg/plate)	revertants number	conclusion
3c	0.0	8.5 ± 2.5	no mutagenic
	27.9	8.0 ± 2.0	
	37.2	4.5 ± 2.0	
	55.8	5.0 ± 0.5	
	111.7	8.0 ± 1.0	
	335.0	9.5 ± 0.5	
positive control (NPD)	20.0	394.0 ± 10	mutagenic

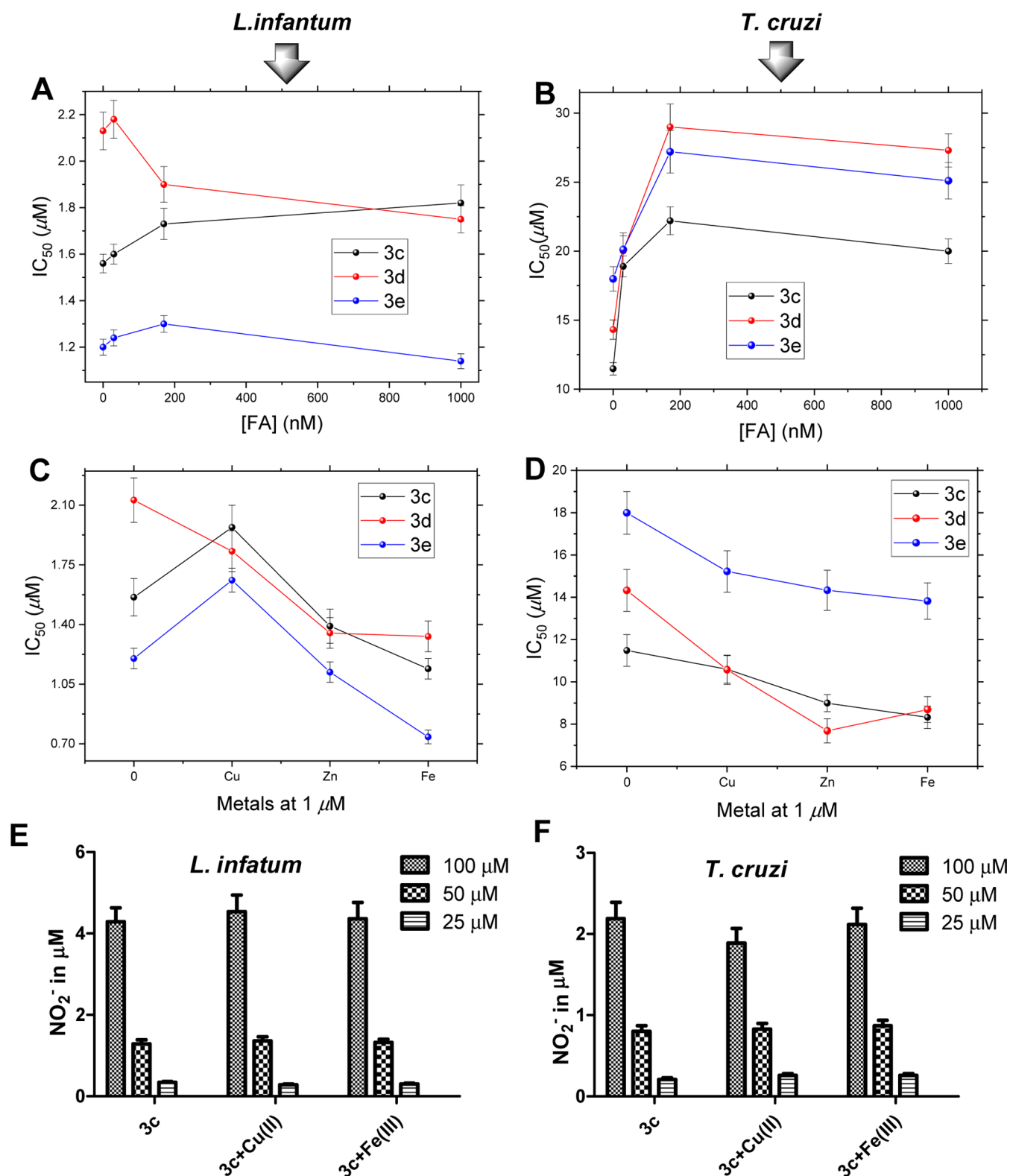
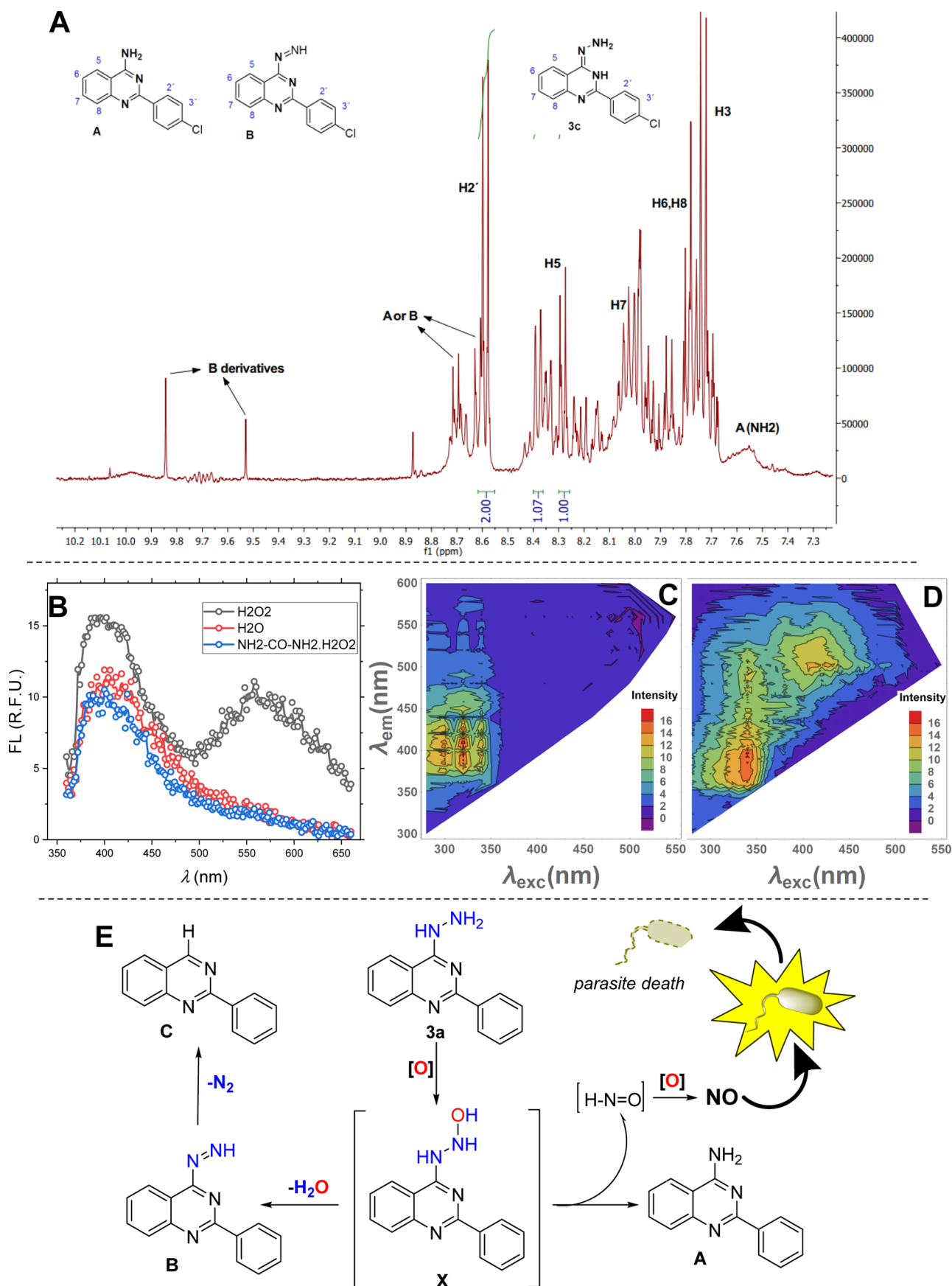


Figure 2. In vitro efficacy (IC₅₀) of 3c, 3d, and 3e on promastigotes of *L. infantum* (A) and epimastigotes of *T. cruzi* (B) in the absence and presence of FA. In vitro efficacy (IC₅₀) of 3c, 3d, and 3e for *L. infantum* promastigotes (C) and *T. cruzi* epimastigotes (D) in the absence and presence of Cu(II), Fe(III), and Zn(II) cations. Concentrations of the nitrite ion (in μM) from treated *L. infantum* promastigotes (E) and *T. cruzi* epimastigotes with 3c (F).

273 oxidative decomposition of the hydrazine moiety. Regarding
 274 the antifolate pathway, there are many quinazoline derivatives
 275 based on that mechanism.⁴² From an indirect strategy,³² we
 276 evaluated the antifolate activity of the compounds 3c, 3d, and

3e through the measurement of IC₅₀ against axenic parasites in
 the presence or absence of D,L-folic acid (FA) (Figure 2A,B). If
 an antifolate activity is involved in the anti-trypansomatid
 activity of the 2-arylquinazolines, an increase in the IC₅₀ of the



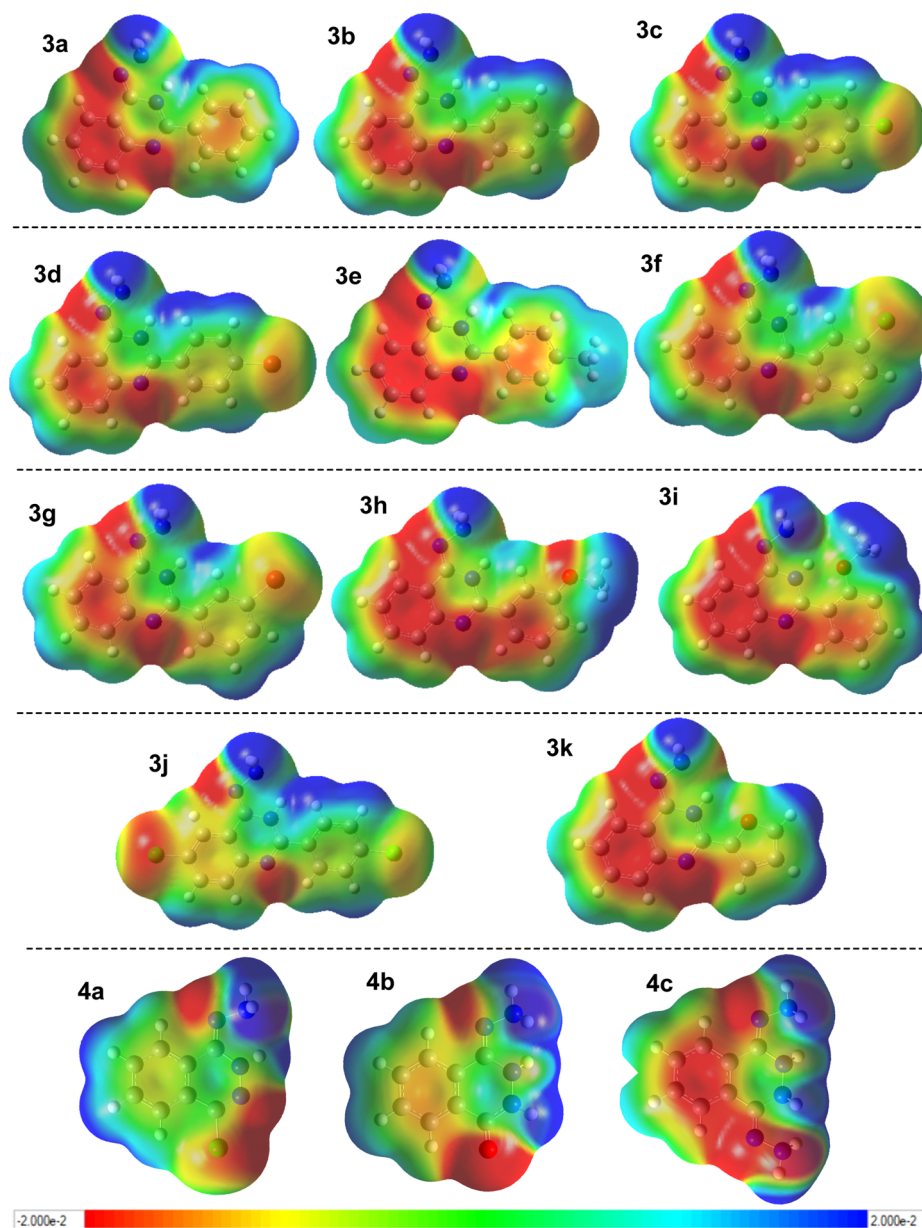


Figure 4. Electrostatic potential surface (EPS) for the 2-arylquinazolin-4-hydrazine **3a–k** and phthalazin-1-hydrazines **4a–c**.

281 derivatives in the presence of FA is expected.³² Increasing IC₅₀
 282 values by about twofold were found with the addition of FA for
 283 treated epimastigote *T. cruzi* with **3c**, **3d**, and **3e** (Figure 2B).
 284 In contrast, the presence of FA displayed a modest increase in
 285 IC₅₀ for treated *Leishmania*, in particular, for **3c** (Figure 2A).
 286 Conversely, IC₅₀ of miltefosine and nifurtimox was not affected
 287 by the addition of FA to the treated parasites. Then, we
 288 concluded that the anti-epimastigote response of **3c**, **3d**, and **3e**
 289 could be derived from an antifolate activity, whereas the
 290 significant leishmanicidal activity of them seems to be
 291 attributed primarily to an alternative mechanism, the antifolate
 292 activity being a secondary mechanism for *Leishmania*.

293 Next, we explored the role of the NO production in the
 294 antitrypanosomatid activity of active 2-arylquinazolin-4-hydra-
 295 zines. Furthermore, we studied the effect of some polyvalent
 296 transition metals (Fe³⁺, Cu²⁺, and Zn²⁺) in the biological
 297 activity and modulation of NO release. For them, we
 298 performed separately four experiments: (i) anti-trypanosoma-
 299 tid activity of **3c**, **3d**, and **3e** in the presence of transition

metallic cations; (ii) NO-production in treated parasites in the 300
 absence and presence of metallic cations; (iii) tentative 301
 decomposition of the hydrazine moiety in **3c** or **3h** through 302
 spectroscopic experiments; and (iv) theoretical study based on 303
 the HOMO–LUMO orbitals and electrostatic potential 304
 surface (EPS) to distinguish the oxidation ability of the 305
 hydrazine moiety. 306

Due to the high susceptibility of the hydrazine moiety 307
 connected to the electron-deficient ring to the oxidation in the 308
 presence of transition metals,^{17–19} we first evaluated the effect 309
 of the metal cations (at 1 μM) on cell viability of **3c**-, **3d**-, and 310
3e-treated parasites (Figure 2C,D). In general, a moderate 311
 decrease in IC₅₀ values, mainly upon Zn²⁺ and Fe³⁺, was found 312
 for all treated parasites in the presence of transition metals. 313
 Only Cu²⁺ displayed an increase in IC₅₀ values in *Leishmania* 314
 parasites for **3c** and **3e**. 315

With this information, we measured the level of nitrite ions 316
 in parasite culture by the Griess test for non-infective *L.* 317
infantum and *T. cruzi* in the presence or absence of the most 318

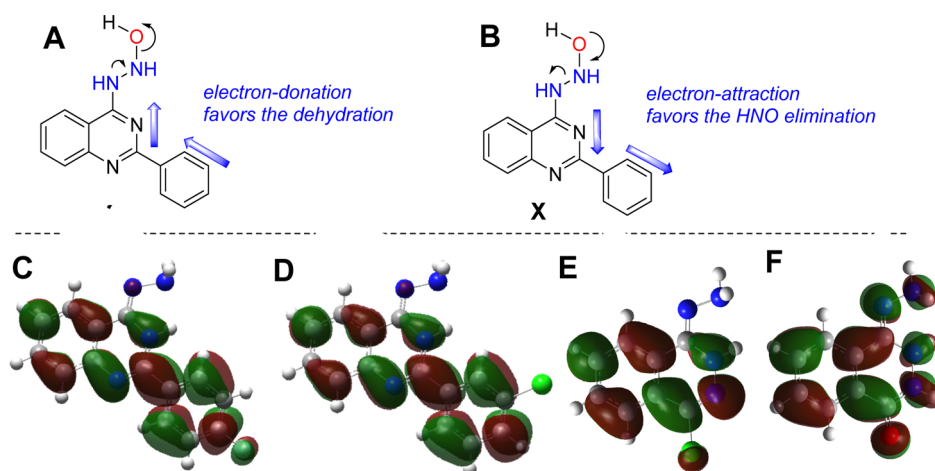


Figure 5. Tentative mechanistic dehydration (A) and HNO-elimination (B) in intermediate X from an electronic point of view and LUMO maps for **3c** (C), **3f** (D), **4a** (E), and **4c** (F).

319 active compound **3c** at different doses (Figure 2E,F).³⁴ Further
 320 measurements in the presence of Cu^{2+} and Fe^{3+} cations were
 321 performed to study whether transition metals mediated NO
 322 production. A control experiment was performed with the 2-
 323 (4-chlorophenyl)quinazolin-4(3H)-one, which was active
 324 against *Leishmania* parasites,³² in order to discard a direct
 325 mediation by the chemical system to activate the nitric oxide
 326 synthase (NOS) enzyme. From results, treated parasites
 327 displayed an appreciable amount of nitrite ion in sub-
 328 micromolar ranges, and its production showed dependence
 329 with the compound doses. No production was detected in the
 330 presence of the 2-(4-chlorophenyl)quinazolin-4(3H)-one,
 331 which suggests that the NO is possibly not generated from
 332 an enzymatic stimulation of the chemical system, opening the
 333 door to the role of the decomposition of hydrazine moiety to
 334 interpret the NO in the 2-arylquinazolin-4-hydrazone. Interest-
 335 ingly, *Leishmania* parasites showed a more significant nitrite
 336 ion production than *T. cruzi* under the same conditions. The
 337 use of Cu^{2+} and Fe^{3+} cations increases discretely the nitrite ion
 338 concentration. This evidence suggests that the 2-aryl-
 339 quinazolin-4-hydrazines could be involved in the production
 340 of NO within parasites, and it could be attributed to chemical
 341 decomposition of hydrazine to NO and organic sub-products.
 342 Meanwhile the cations improved, discretely, the activity of the
 343 active compounds, but they did not seem to play an essential
 344 role in the NO production, its mediation being discarded in
 345 hydrazine decomposition.

346 To demonstrate that the production of NO in treated
 347 parasites was derived from the partial chemical decomposition
 348 of 2-arylquinazolin-4-hydrazone, we performed spectroscopic
 349 studies (NMR and fluorescence) in the absence and presence
 350 of an oxidant (H_2O_2 or $\text{NH}_2\text{-CO-NH}_2\cdot\text{H}_2\text{O}_2$) (Figure 3).
 351 The NMR experiment confirmed that compound **3c** was
 352 decomposed in at least three additional products: 4-amino-2-
 353 arylquinazoline (A), 1-(2-arylquinazolin-4-yl)diazene (B), or
 354 2-arylquinazoline (C) (Figures 3A, S1, and S2). A single peak
 355 by about 9.6 or 9.7 ppm may be associated to the ($-\text{N}=\text{NH}$)
 356 proton in metabolite B, while a broad peak at 7.5 ppm may
 357 belong to the amino proton in metabolite A. Specific peaks at
 358 8.34 and 7.8 ppm are reported in the literature for 4-
 359 aminoquinazolines.⁴³ To support this evidence, we performed
 360 a fluorescence study for the resulting solution, and it was
 361 compared with that solution in the absence of an oxidant. It is

documented that 2-aminoquinazolines present fluorescence
 362 properties with a normal emission at 400–430 nm and a
 363 secondary anomalous at 575–600 nm.^{44–46} It is well known
 364 that the fluorometry is a high-sensitivity technique, which
 365 facilitated the detection of low-concentration compounds.
 366 From the fluorescence experiment, in general, all 2-
 367 arylquinazolin-4-hydrazines showed a maximum normal
 368 emission wavelength at 400 nm (Figures 3B–D and S8 and
 369 S9). Under oxidative conditions, only the compound **3h**
 370 showed an emission spectrum with appreciable changes, being
 371 our model structure. The emission spectrum of **3h** showed the
 372 emergence of an additional anomalous emission peak at 575
 373 nm (Figure 3B). To facilitate the identification of the
 374 anomalous emission band, an emission-excitation matrix
 375 (EEM) plot⁴⁷ was performed, and the anomalous emission
 376 band (575 nm) in combination with the normal emission band
 377 was confirmed for the compound **3h** upon oxidative
 378 conditions. Meanwhile, only the normal emission band was
 379 seen in the absence of the oxidant (Figure 3C,D). The latter
 380 supports the formation of product A, and the solution must
 381 consist of a mixture between starting quinazoline and the
 382 metabolite A. UV–vis spectroscopy did not allow the detection
 383 of the low decomposed products (Figure S5F). With all this
 384 biological and chemical evidence, we proposed a tentative
 385 decomposition pathway for the hydrazine moiety in 2-
 386 arylquinazolin-4-hydrazone with NO releasing from parasite
 387 culture (Figure 3E). Initially, 2-arylquinazolin-4-hydrazone is
 388 oxidized within parasites to form intermediate X. Subsequently,
 389 X may suffer: (i) a dehydration leading B and (ii) a
 390 decomposition of the hydroxylhydrazinyl moiety to form
 391 product A and H–NO. This last species could be oxidized to
 392 NO through the Fe(II)-O_2 complex, which is present in the
 393 SOD enzyme of trypanosomatids.⁴⁸
 394

In order to understand theoretically the origin of the
 395 tentative decomposition of the hydrazine moiety in 2-
 396 arylquinazolin-4-hydrazone, we analyzed its HOMO–LUMO
 397 and EPS. From EPS (Figure 4), it should be noted primarily
 398 that the imine-tautomer presented a more negative electron
 399 density on bonded nitrogen (more red color in EPS map) to
 400 the heterocyclic ring than hydrazine-tautomer; thus, the imine-
 401 tautomer is more suitable to suffer oxidation than the
 402 hydrazine-tautomer in the studied 2-arylquinazoline/phthala-
 403 zin-hydrazines (compare Figure 4 vs Figure S14). Comparison
 404

405 between the 2-arylquinazolin with phthalazin-hydrazines
406 showed that the first presented a more negative bonded
407 nitrogen to the heterocyclic ring than the phthalazine analogue,
408 although these differences are smaller, which supposes a higher
409 nucleophilic character in the terminal amino of hydrazine of 2-
410 arylquinazoline than in the phthalazine-hydrazine. It is highly
411 required to form metabolite X (Figure 3E). Thus, from the
412 electronic point of view, the nucleophilic addition of the amino
413 terminal to the oxidant for the formation of X is more favored
414 in the 2-arylquinazolin-hydrazine than phthalazin-hydrazines.
415 Within the 2-arylquinazolin-4-hydrazines, no appreciable
416 differences were noted from the electronic density point of
417 view, but some important differences were noted on the
418 quinazoline core. A lower electron density was seen on the
419 benzo-core of the 2-arylquinazoline bearing the electron-
420 deficient aryl moiety (3b, 3c, 3d, 3f, 3g, and 3j) than on those
421 bearing the electron-rich moiety (3a, 3e, 3h, 3i and 3k). The
422 electron-deficient nature of the quinazoline core could be an
423 important electronic feature to favor the decomposition of X to
424 form A with release of HNO because this transformation
425 mechanistically required that the quinazoline core acts as an
426 electron acceptor. It favors the electronic movement from the
427 hydroxyl moiety to bonded nitrogen to form H–NO (Figure
428 5A). In contrast, a higher electronic density on the quinazoline
429 core was given to the system in an electron donor to favor the
430 dehydration of X via an electron movement from pyrimidyl to
431 the hydrazine moiety (Figure 5B). From HOMO–LUMO,
432 LUMO maps showed that an electron transfer (ET) from the
433 heterocyclic core to the hydrazine moiety is more suitable in
434 the phthalazine-hydrazine than in the 2-arylquinazolines
435 (Figures 5C–F and S6–S13), supporting the fact that the 2-
436 arylquinazoline is a more convenient scaffold to favor the
437 required electronic movement from hydrazine to the quinazo-
438 line ring for decomposition of hydrazine to release HNO
439 (Figure 5A,B). Further HOMO–LUMO data and graphical
440 orbitals can be found in the Supporting Information.

441 In summary, we showed the potential of a hydrazine as a
442 pharmacophore for the construction of a new type of
443 antitrypanosomal agent based on its feasible oxidative
444 decomposition to release NO in electron-deficient systems
445 and the high toxicity of this small molecule against
446 trypanosomatids. Then, a series of 2-arylquinazolin-4-hydra-
447 zines were synthesized, and some of the derivatives, 3b, 3c, and
448 3f, showed a good in vitro activity against non-infective and
449 infective strains of *Leishmania* and against non-infective strain
450 of *T. cruzi*, lower cytotoxicity against different macrophages,
451 high selectivity indexes over 10 units, and non-mutagenic
452 effects. Interestingly, studies of the mechanism of action
453 suggested that the production of NO could be one of the
454 responsible anti-trypanosomatid activities of the 2-arylquina-
455 zolin-4-hydrazines, in combination with a discrete contribution
456 of antifolate activity. Chemical experiments based on
457 spectroscopic measurements identified that the formation of
458 the subproduct under oxidative environments in conjunction
459 with biological NO releasing from treated parasites allowed us
460 to propose a mechanistic decomposition of the hydrazine
461 moiety to form NO. Finally, theoretical calculations based on
462 HOMO–LUMO and EPS analysis showed that the feasible
463 oxidative decomposition of the hydrazine moiety in 2-
464 arylquinazolines depended on two electronic conditions: (i)
465 to guarantee a high electron density on the bonded nitrogen of
466 the hydrazine moiety and, at the same time, (ii) a strong
467 electron attraction from hydrazine to the heterocyclic ring with

a nucle ET process. It was consistently achieved for the 2- 468
arylquinazolin-4-hydrazine over, for example, phthalazin-1- 469
hydrazine, and it showed to be modulated by the incorporation 470
of electron-deficient aryl moieties. All the evidence allowed us 471
to explain the significant biological activity of the electron-aryl- 472
deficient 2-arylquinazolin-4-hydrazine, and our investigation 473
opens a new perspective for the design of effective and safe 474
NO-donors with anti-trypanosomatid activities. 475

476 ■ METHODS

General Chemistry. 2-Arylquinazolin-4(3H)-ones 1a–k 477
were previously prepared.³² The rest of the reagents were 478
purchased from commercial sources and used without further 479
purification. Solvents were anhydrous HPLC grade. ¹H NMR 480
and ¹³C NMR spectra were recorded on a 400 MHz NMR- 481
spectrometer (Bruker-400) or 250 MHz NMR-spectrometer 482
JEOL. Multiplicity is indicated as follows: s (singlet), d 483
(doublet), t (triplet), m (multiplet), dd (doublet of doublets), 484
and brs (broad singlet); chemical shifts were measured in parts 485
per million (δ), and coupling constants (*J*) are given in Hz. 486
Proton chemical shifts were given relative to tetramethylsilane 487
(δ 0.00 ppm) in CDCl₃ or DMSO-*d*₆. Carbon chemical shifts 488
are internally referenced to the deuterated solvent signals in 489
CDCl₃ (δ 77.00 ppm) or DMSO-*d*₆ (δ 40.02 ppm). Elemental 490
analyses of the synthesized compounds were performed using a 491
PerkinElmer 2400 CHN analyzer: results fell in the range of 492
0.4% of the required theoretical values. TLC was performed 493
using commercially available 100–400 mesh silica gel plates 494
(GF254) and visualized under UV light (at 254 nm). 495
Absorption and fluorescence spectral data were obtained 496
from a Thermo Scientific Varioskan Flash Multimode 497
instrument for air-equilibrated solutions at 25 °C. EEM plots 498
were obtained as described previously (Figures S4 and S5).⁴⁷ 499

**General Procedure for Synthesis of 2-Arylquinazoli- 500
4-hydrazines.** The corresponding starting materials 1a–k 501
(0.5 mmol, 1.0 equiv) were mixed with POCl₃ (6 equiv) 502
according to the reported protocol with a few modifica- 503
tions.^{34,35} The reaction mixture was stirred for 4–6 h at 100 504
°C. It was monitored by TLC. The reaction mixture was 505
quenched with water at 0 °C with dichloromethane (3 × 20 506
mL). The combined organic extracts were washed with 507
saturated aqueous NaCl solution, dried over anhydrous 508
Na₂SO₄, and filtered. The mixture was passed by a flash 509
chromatographic column to obtain the intermediates 2a–k. 510
The isolated product was used for the next reaction step. Then, 511
to a hot hydrazine hydrate (4 equiv) solution in ethanol was 512
added the intermediates 2a–k (1 equiv) at 0.1 M 513
concentration and heated at 70 °C for 2 h. The reaction was 514
monitored by TLC. The reaction mixture was cooled at 0 °C, 515
and then, the resulting solid was filtered by vacuum to give 516
from a pale yellow to orange solid. The isolated solid was 517
recrystallized with cold ethanol to yield the pure product. The 518
product were characterized by NMR spectroscopy. Detailed 519
spectroscopic data and spectra can be found in the Supporting 520
Information. 521

In Vitro Anti-*T. cruzi* Evaluation on Epimastigotes. 522
The effect of the studied compounds on the epimastigote 523
viability of *T. cruzi* (CL Brener clone) was determined through 524
the turbidimetric technique.³⁶ Stock solutions (at 3000 μ M) of 525
the tested compounds in DMSO were prepared. Fresh 526
solutions were diluted in the culture medium to obtain the 527
different concentrations from 0.5 to 25 μ M. All controls and 528
tested well contain no more than 1% of DMSO. The screening 529

530 was performed in 24-well microliter plates maintained at 25
531 °C. Briefly, 2×10^6 parasites/mL were exposed to increasing
532 concentrations from 0.5 to 25.0 μM (1.0, 5.0, 10.0, 20.0, and
533 50.0 μM) of each compound for 120 h at 25 °C. The biological
534 effect of these compounds was evaluated through absorbance
535 measurements at 595 nm using a spectrometer EL301
536 microwell at 5 days. Untreated control parasites were used to
537 calculate the relative proliferation. Nifurtimox was used as a
538 reference drug. The percentage of growth inhibition (PGI) was
539 determined as follows: $\text{PGI} (\%) = \{1 - [(A_p - A_{0p}) / (A_c -$
540 $A_{0c})]\} \times -100$, where $A_p = A_{595}$ of the culture containing the
541 compound at day 5; $A_{0p} = A_{595}$ of the culture containing the
542 compound at day 0; $A_c = A_{595}$ of the culture in the absence of
543 any drug (control) at day 5; and $A_{0c} = A_{595}$ in the absence of
544 any drug at day 0.

545 To determine IC_{50} values, PGI was followed of increasing
546 concentrations of the corresponding agent. The IC_{50} was taken
547 as the concentration of the agent needed to reduce the PGI to
548 50%.

549 **In Vitro Anti-Leishmania Evaluation on Promasti-**
550 **gotes.** The cell viability of 2-aryl-quinazolin-4-hydrazines **3a–**
551 **k** on *Leishmania infantum* (MHOM MA6717MAP263) strain
552 was assessed using the 3-(4,5-dimethylthiazol-2-yl)-2,5-diphe-
553 nyltetrazolium bromide (MTT) assays with a few modifica-
554 tions.³⁴ Stock solutions (at 3000 μM) of the tested compounds
555 in DMSO were prepared. Fresh solutions were diluted in the
556 culture medium to obtain the different concentrations from 0.5
557 to 25 μM . All controls and tested well contain no more than
558 1% of DMSO. The screening was performed in 96-well
559 microliter plates maintained at 25 °C. Briefly, 2×10^6
560 parasites/mL were exposed to increasing concentrations from
561 0.5 to 25.0 μM (1.0, 5.0, 10.0, 20.0, and 50.0 μM) of each
562 compound for 72 h at 25 °C. Controls contain 1% of DMSO
563 and medium. After incubation, cells were treated with 100 μL
564 0.4 mg/mL MTT for 4 h at 37 °C. Subsequently, the medium
565 was removed, and 100 μL of DMSO was added to the resulting
566 mixture to dissolved formazan salt. The solubilized formazan
567 product was quantified through absorbance measurements at
568 570 nm using a Thermo Scientific Varioskan Flash Multimode
569 instrument at 72 h. Miltefosine and glucantime were used as
570 reference drugs. Untreated control parasites were used to
571 calculate the relative proliferation. The percentage of parasite
572 inhibition with regard to controls was calculated as $= 100 -$
573 $[(\text{parasite counts in treated cells} / \text{parasite counts in untreated}$
574 $\text{cells}) - 100]$.

575 **Ex Vivo Antiamastigote Activity of *L. Braziliensis*.**
576 Intracellular amastigotes were directly extracted from footpad
577 lesions in BALB/c mice previously infected with *L. braziliensis*
578 (MHOM/BZ/82/M2903). The isolate contained amastigotes
579 and small portions of infected macrophages and macrophages.
580 These two last portions were removed from the cellular
581 mixture by controlled centrifugation (at 3000 rpm by 2–3
582 min) to obtain a culture enough pure in amastigotes.^{32,35,49,50}
583 Amastigote culture was maintained at 37 °C and pH 5.5 in
584 M199 medium (Invitrogen, Leiden, The Netherlands)
585 supplemented with 10% heat-inactivated FCS, 1 g/L L-alanine,
586 100 mg/L L-asparagine, 200 mg/L sucrose, 50 mg/L sodium
587 pyruvate, 320 mg/L malic acid, 40 mg/L fumaric acid, 70 mg/
588 L succinic acid, 200 mg/L α -ketoglutaric acid, 300 mg/L citric
589 acid, 1.1 g/L sodium bicarbonate, 5 g/L 2-(N-morpholino)
590 ethanesulfonic acid (MES), 0.4 mg/L hemin, and 10 mg/L
591 gentamicin. The screening was performed in 96-well microtiter
592 plates maintained at 37 °C. Briefly, 2×10^6 parasites/mL were

593 exposed to increasing concentrations between 1.0 and 50.0 μM
594 (1.0, 5.0, 10.0, 20.0, and 50.0 μM) of each compound **3a–f**.
595 Controls contained 1% DMSO. Miltefosine and glucantime
596 were used as reference drugs. The effect of the compound
597 against amastigote forms was tested at 48 h using conventional
598 counting parasites in a Neubauer chamber (optical microscopy,
599 1000 \times magnification). Untreated control parasites were used
600 to calculate the relative proliferation.

Cytotoxicity. Peritoneal and J774.1A macrophages were
601 grown in DMEM medium supplemented with 10% heat-
602 inactivated fetal bovine serum, 1% L-glutamine, 1% strepto-
603 mycin, and 100 units/mL penicillin. Cell viability was assessed
604 using the MTT protocol.³² Stock solutions (at 25,000 μM) of
605 the tested compounds in DMSO were prepared. Cells were
606 grown in 96-well plates (5×10^4 cells/well) for 24 h. Cultures
607 were carried out at 37 °C in a humidified atmosphere with 5%
608 CO_2 and incubated with the compounds **3a**, **3b**, **3c**, **3d**, **3e**,
609 and **3f** at 10.0, 25.0, 50.0, 75, and 100 μM concentrations for
610 48 h. After incubation, the medium was removed, and the cells
611 were treated with 100 μL of 0.4 mg/mL MTT for 4 h at 37 °C.
612 Subsequently, 100 μL of DMSO was added to the mixture.
613 The solubilized formazan product was quantified through
614 absorbance measurements at 570 nm. The absorbance values
615 were transformed to the percentage of cytotoxicity compared
616 to the negative controls.
617

Statistical Analysis. All biological experiments were
618 performed at least three times. The results are expressed as
619 mean \pm SD. The Anova test were performed. Only post hoc
620 Dunnet test $p < 0.01$ was considered to be statistically
621 significant. The dose–response curves were plotted using
622 GraphPad prism v.5.02 software.
623

Mutagenicity Ames Test.⁴¹ In vitro genetic toxicity
624 *Salmonella typhimurium* TA 98 strain was incubated in agar
625 minimum glucose milieu solution (Difco BactoR agar) and
626 aqueous glucose solution (40%). The direct toxicity of the
627 compound **3c** against *S. typhimurium* TA 98 strain was studied.
628 From these data, the mutagenic assay was performed by
629 incubating **3c** in phosphate buffer (0.1 M, pH 7.4) and DMSO
630 (10% v/v) at six doses, 0.0, 27.9, 37.2, 55.8, 111.7, and 335 $\mu\text{g}/$
631 plate. The control positive consisted of NPD (20.0 mg/plate),
632 and negative controls consisted of phosphate buffer and
633 DMSO (10% v/v) (0.0 $\mu\text{g}/$ plate of **3c**) solutions. The
634 revertant numbers were counted, and the studied system was
635 considered mutagenic if the colony number was at least double
636 the natural revertants (negative control) for two or more
637 consecutive doses.
638

Determination of Nitrite Concentration. Nitrite
639 (NO_2^-) accumulation was determined in supernatants of
640 promastigote or epimastigote culture (5×10^6 parasites/well),
641 which were incubated for 5 days in the presence of the active
642 **3c** at increasing concentrations (25, 50, and 100 μM). Three
643 wells with untreated parasites were incubated as the negative
644 control. The assay was performed by the Griess reaction
645 (detection limit: 1.56 μM) with sodium nitrite as a standard as
646 previously described.³⁴ In brief, 100 μL of Griess reagent 1%
647 sulfanilamide in 50% of acetic acid was added to 400 μL of
648 each sample. The blank reference and standard curve were
649 determined. After 15 min, 100 μL of a solution of *N*-
650 [naphthyl]ethylenediamine dihydrochloride (1%) in acetic
651 acid in 50% was added. The absorbance was measured at 540
652 nm for that resulting final solution. Nitrite content was
653 quantified by the extrapolation from the sodium nitrite
654 standard curve in each experiment. All the assays were 655

656 performed by triplicate. The results were expressed as the
657 amount of nitrite ion (in μM).

658 **Effect of Polyvalent Cations and Folic Acid.** These
659 were performed following the protocols of cell viability of
660 promastigote *Leishmania* and epimastigote *T. cruzi*. Details are
661 shown in the [Supporting Information](#).

662 **Theoretical Calculations.** All theoretical calculations, in
663 the gas phase, were performed using the B3LYP functional⁵¹ in
664 conjunction with the 6-31G(d,p) basis set⁵² using Gaussian09
665 quantum chemistry software.⁵³ The geometry of all tested
666 compounds were optimized, and HOMO–LUMO orbital
667 frontiers and EPS were obtained. Theoretical calculations were
668 performed according to the reported strategy for similar
669 structures.⁵⁴ HOMO and LUMO frontier orbital maps for
670 compounds and data are shown in [Figures S6–S9](#) and [Table](#)
671 [S2](#).

672 ■ ASSOCIATED CONTENT

673 ■ Supporting Information

674 The Supporting Information is available free of charge at
675 <https://pubs.acs.org/doi/10.1021/acsomega.2c06455>.

676 Full experimental details, emission spectra in the
677 presence of tested acids and their corresponding
678 Stern–Volmer plots, and theoretical data (PDF)

679 ■ AUTHOR INFORMATION

680 Corresponding Authors

681 **Angel H. Romero** – Grupo de Química Orgánica Medicinal,
682 Instituto de Química Biológica, Facultad de Ciencias,
683 Universidad de la Republica, Montevideo 11400, Uruguay;
684 Laboratorio de Ingeniería Genética, Instituto de Biomedicina,
685 Facultad de Medicina, Universidad Central de Venezuela,
686 Caracas 1073, Venezuela; orcid.org/0000-0001-8747-5153;
687 Email: angel.ucv.usb@gmail.com

688 **Hugo Cerecetto** – Grupo de Química Orgánica Medicinal,
689 Instituto de Química Biológica, Facultad de Ciencias,
690 Universidad de la Republica, Montevideo 11400, Uruguay;
691 Area de Radiofarmacia, Centro de Investigaciones Nucleares,
692 Facultad de Ciencias, Universidad de la Republica,
693 Montevideo 11400, Uruguay; orcid.org/0000-0003-1256-3786;
694 Email: hcerecetto@cin.edu.uy

695 Authors

696 **Elena Aguilera** – Grupo de Química Orgánica Medicinal,
697 Instituto de Química Biológica, Facultad de Ciencias,
698 Universidad de la Republica, Montevideo 11400, Uruguay

699 **Lourdes Gotopo** – Laboratorio de Síntesis de Orgánica,
700 Facultad de Ciencias, Universidad Central de Venezuela,
701 Caracas 1041-A, Venezuela

702 **Jaime Charris** – Laboratorio de Síntesis de Medicamentos,
703 Facultad de Farmacia, Universidad Central de Venezuela,
704 Caracas 1041-A, Venezuela

705 **Noris Rodríguez** – Laboratorio de Ingeniería Genética,
706 Instituto de Biomedicina, Facultad de Medicina, Universidad
707 Central de Venezuela, Caracas 1073, Venezuela

708 **Henry Oviedo** – Laboratorio de Ingeniería Genética, Instituto
709 de Biomedicina, Facultad de Medicina, Universidad Central
710 de Venezuela, Caracas 1073, Venezuela

711 **Belén Dávila** – Grupo de Química Orgánica Medicinal,
712 Instituto de Química Biológica, Facultad de Ciencias,
713 Universidad de la Republica, Montevideo 11400, Uruguay

Gustavo Cabrera – Laboratorio de Síntesis de Orgánica, 714
715 Facultad de Ciencias, Universidad Central de Venezuela,
716 Caracas 1041-A, Venezuela

Complete contact information is available at: 717
<https://pubs.acs.org/doi/10.1021/acsomega.2c06455> 718

719 Author Contributions

A.H.R. performed synthetic experiments and assays for *L.* 720
braziliensis and chemical mechanistic studies, organized the 721
investigation, analyzed the experimental and theoretical data, 722
and prepared and revised the manuscript. E.A. performed 723
biological experiments relative to *L. infantum* and *T. cruzi* and 724
mechanistic biological studies. B.D. performed the Ames Test. 725
L.A.G. performed theoretical experiments. H.O. prepared 726
cultures for in vitro *L. braziliensis* assays. G.C., J.C., N.R., 727
and H.C. provided financial resources. H.C. supervised 728
investigation. H.C. and J.C. revised the manuscript. All authors 729
have given approval to the final version of the manuscript. 730

731 Notes

The authors declare no competing financial interest. 732

733 ■ ACKNOWLEDGMENTS

A.H.R. thanks Agencia Nacional de Investigación e Innovación 734
(ANII) (Uruguay) and CDCH-UCV (Venezuela) for financial 735
support under grant codes PD_NAC_2018_1_150515 and 736
PG-09-8819/2013, respectively. A.H.R., H.C., and E.A. thank 737
further resources from PEDECIBA-QUIMICA (Uruguay) and 738
SNI-ANII (Uruguay). The authors thank Horacio Perazoglo 739
(NMR Laboratory, Universidad de la República) and Dr. Erick 740
Castro (Instituto de Física da UFRGS, Brazil) for NMR 741
spectra and construction of EMM-3D correlations, respec- 742
tively. Also, the authors are grateful to Copernico Cluster 743
(Universidad Central Venezuela, Caracas, Venezuela) for 744
facilitating calculation. 745

746 ■ REFERENCES

- 747 (1) Kaufer, A.; Ellis, J.; Stark, D.; Barratt, J. The evolution of
748 trypanosomatid taxonomy. *Parasites Vectors* **2017**, *10*, 287.
- 749 (2) CDC Global Health. *Infographics-Antibiotic Resistance The Global*
750 *Threat*.
- 751 (3) World Health Organization. Leishmaniasis, [https://www.who.](https://www.who.int/news-room/fact-sheets/detail/leishmaniasis)
752 [int/news-room/fact-sheets/detail/leishmaniasis](https://www.who.int/news-room/fact-sheets/detail/leishmaniasis).
- 753 (4) Nwaka, S.; Ridley, R. G. Virtual drug discovery and development
754 for neglected diseases through public-private partnerships. *Nat. Rev.*
755 *Drug Discovery* **2003**, *2*, 919–928.
- 756 (5) (a) Ascenzi, P.; Bocedi, A.; Gradoni, L. The Anti-Parasitic
757 Effects of Nitric Oxide. *IUBMB Life* **2003**, *55*, 573–578. (b) Pavanelli,
758 W. R.; Nogueira Silva, J. J. The Role of Nitric Oxide in Immune
759 Response Against Trypanosoma Cruzi Infection. *Open Nitric Oxide J.*
760 **2010**, *2*, 1–6.
- 761 (6) Carneiro, P. P.; Conceição, J.; Macedo, M.; Magalhães, V.;
762 Carvalho, E. M.; Bacellar, O. The Role of Nitric Oxide and Reactive
763 Oxygen Species in the Killing of *Leishmania braziliensis* by
764 Monocytes from Patients with Cutaneous Leishmaniasis. *PLoS One*
765 **2016**, *11*, No. e0148084.
- 766 (7) Almeida-Souza, F.; da Silva, V.; Taniwaki, N. N.; Hardoim, D.;
767 Mendonça Filho, A. R.; Moreira, W. F.; Buarque, C.; Calabrese, K.;
768 Abreu-Silva, A. L. Nitric Oxide Induction in Peritoneal Macrophages
769 by a 1,2,3-Triazole Derivative Improves Its Efficacy upon *Leishmania*
770 *amazonensis* In Vitro Infection. *J. Med. Chem.* **2021**, *64*, 12691–
771 12704.
- 772 (8) Genestra, M.; Soares-Bezerra, R. J.; Gomes-Silva, L. In vitro
773 sodium nitroprusside-mediated toxicity towards *Leishmania amazo-*
774 *nensis* promastigotes and axenic amastigotes. *Cell Biochem. Funct.*
775 **2008**, *26*, 709–717.

- 776 (9) Melo Pereira, J. C.; Carregaro, V.; Costa, D. L.; Santana da Silva,
777 J.; Cunha, F. Q.; Franco, D. W. Antileishmanial activity of
778 ruthenium(II)tetraammine nitrosyl complexes. *Eur. J. Med. Chem.*
779 **2010**, *45*, 4180–4187.
- 780 (10) Silva, J. J. N.; Pavanelli, W. R.; Pereira, J. C. M.; Silva, J. S.;
781 Franco, D. W. Experimental Chemotherapy against *Trypanosoma*
782 *cruzi* Infection Using Ruthenium Nitric Oxide Donors. *Antimicrob.*
783 *Agents Chemother.* **2009**, *53*, 4414–4421.
- 784 (11) Silva, J. J. N.; Guedes, P. M. M.; Zottis, A.; Balliano, T. L.;
785 Nascimento Silva, F. O.; França Lopes, L. G.; Ellena, J.; Oliva, G.;
786 Andricopulo, A. D.; Franco, D. W.; Silva, J. S. Novel ruthenium
787 complexes as potential drugs for Chagas's disease: enzyme inhibition
788 and in vitro/in vivo trypanocidal activity. *Br. J. Pharmacol.* **2010**, *160*,
789 260–269.
- 790 (12) Fershtat, L. L.; Zhilin, E. S. Recent Advances in the Synthesis
791 and Biomedical Applications of Heterocyclic NO-Donors. *Molecules*
792 **2021**, *26*, S705.
- 793 (13) Boiani, L.; Aguirre, G.; González, M.; Cerecetto, H.;
794 Chidichimo, A.; Cazzulo, J. J.; Bertinaria, M.; Guglielmo, S. Furoxan-,
795 alkylnitrate-derivatives and related compounds as anti-trypanosomatid
796 agents: Mechanism of action studies. *Bioorg. Med. Chem.* **2008**, *16*,
797 7900–7907.
- 798 (14) Hernández, P.; Cabrera, M.; Lavaggi, M. L.; Celano, L.;
799 Tiscornia, I.; Rodrigues da Costa, T.; Thomson, L.; Bollati-Fogolin,
800 M.; Miranda, A. L.; Lima, L. M.; Barreiro, E. J.; González, M.;
801 Cerecetto, H. Discovery of new orally effective analgesic and anti-
802 inflammatory hybrid furoxanyl N-acylhydrazone derivatives. *Bioorg.*
803 *Med. Chem.* **2012**, *20*, 2158–2171.
- 804 (15) Hernández, P.; Rojas, R.; Gilman, R. H.; Sauvain, M.; Lima, L.
805 M.; Barreiro, E. J.; González, M.; Cerecetto, H. Hybrid furoxanyl N-
806 acylhydrazone derivatives as hits for the development of neglected
807 diseases drug candidates. *Eur. J. Med. Chem.* **2013**, *59*, 64–74.
- 808 (16) Rehse, K.; Shahrouri, T. Hydrazone Derivatives. *Arch. Pharm.*
809 **1998**, *331*, 308–312.
- 810 (17) Jasch, H.; Scheumann, J.; Heinrich, M. R. Regioselective
811 Radical Arylation of Anilines with Arylhydrazines. *J. Org. Chem.* **2012**,
812 *77*, 10699–10706.
- 813 (18) Zhang, C.; Jiao, N. Copper-Catalyzed Aerobic Oxidative
814 Dehydrogenative Coupling of Anilines Leading to Aromatic Azo
815 Compounds using Dioxxygen as an Oxidant. *Angew. Chem., Int. Ed.*
816 **2010**, *49*, 6174–6177.
- 817 (19) Kindt, S.; Jasch, H.; Heinrich, M. R. Manganese(IV)-mediated
818 hydroperoxyarylation of alkenes with aryl hydrazines and dioxxygen
819 from air. *Chem.—Eur. J.* **2014**, *20*, 6251–6255.
- 820 (20) Kimball, K. F. The mutagenicity of hydrazine and some of its
821 derivatives. *Mutat. Res.* **1977**, *39*, 111–126.
- 822 (21) Smith, G. F. Designing Drugs to Avoid Toxicity. *Prog. Med.*
823 *Chem.* **2011**, *50*, 1–47.
- 824 (22) Narang, R.; Narasimhan, B.; Sharma, S. A review on biological
825 activities and chemical synthesis of hydrazide derivatives. *Curr. Med.*
826 *Chem.* **2012**, *19*, 569–612.
- 827 (23) Le Goff, G.; Ouazzani, J. Natural hydrazine-containing
828 compounds: Biosynthesis, isolation, biological activities and synthesis.
829 *Bioorg. Med. Chem.* **2014**, *22*, 6529–6544.
- 830 (24) Blair, L. M.; Sperry, J. J. Natural products containing a
831 nitrogen-nitrogen bond. *Nat. Prod.* **2013**, *76*, 794–812.
- 832 (25) Burke, A. A.; Severson, E. S.; Mool, S.; Solares Bucaro, M. J.;
833 Greenaway, F. T.; Jakobsche, C. E. Comparing hydrazine-derived
834 reactive groups as inhibitors of quinone-dependent amine oxidases. *J.*
835 *Enzyme Inhib. Med. Chem.* **2017**, *32*, 496–503.
- 836 (26) Hampannavar, G. A.; Karpoormath, R.; Palkar, M. B.; Shaikh,
837 M. S.; Chandrasekaran, B. Dehydrozingerone Inspired Styryl
838 Hydrazone Thiazole Hybrids as Promising Class of Antimycobacterial
839 Agents. *ACS Med. Chem. Lett.* **2016**, *7*, 686–691.
- 840 (27) Ahn, J. H.; Shin, M. S.; Jun, M. A.; Jung, S. H.; Kang, S. K.;
841 Kim, K. R.; Rhee, S. D.; Kang, N. S.; Kim, S. Y.; Sohn, S. K.; Kim, S. G.;
842 Jin, M. S.; Lee, J. O.; Cheon, H. G.; Kim, S. S. Synthesis, biological
843 evaluation and structural determination of β -aminoacyl-containing
cyclic hydrazine derivatives as dipeptidyl peptidase IV (DPP-IV) 844
inhibitors. *Bioorg. Med. Chem. Lett.* **2007**, *17*, 2622–2628. 845
- (28) Dascalu, A. E.; Ghinet, A.; Lipka, E.; Furman, C.; Rigo, B.; 846
Fayeulle, A.; Billamboz, M. Design, synthesis and evaluation of 847
hydrazine and acyl hydrazone derivatives of 5-pyrrolidin-2-one as 848
antifungal agents. *Bioorg. Med. Chem. Lett.* **2020**, *30*, 127220. 849
- (29) Dehghani, Z.; Khoshneviszadeh, M.; Khoshneviszadeh, M.; 850
Ranjbar, S. Veratric acid derivatives containing benzylidene-hydrazine 851
moieties as promising tyrosinase inhibitors and free radical scavengers. 852
Bioorg. Med. Chem. **2019**, *27*, 2644–2651. 853
- (30) Quiliano, M.; Pabón, A.; Ramirez-Calderon, G.; Barea, C.; 854
Deharo, E.; Galiano, S.; Aldana, I. New hydrazine and hydrazide 855
quinoxaline 1,4-di-N-oxide derivatives: In silico ADMET, antiplasmo- 856
dial and antileishmanial activity. *Bioorg. Med. Chem. Lett.* **2017**, *27*, 857
1820–1825. 858
- (31) Soares, R. R.; Antinarelli, L. L.; Souza, V. F.; Souza, F.; Lopes, 859
K. G.; Scopel, S.; Coimbra, D.; Silva, C.; Abramo, C. In Vivo 860
Antimalarial and In Vitro Antileishmanial Activity of 4- Aminoquinoline 861
Derivatives Hybridized to Isoniazid or Sulfa or Hydrazone 862
Groups. *Let. Drug Des. Discovery* **2017**, *14*, 597–604. 863
- (32) Romero, A. H.; Rodríguez, N.; Oviedo, H. 2-Aryl-quinazolin- 864
4(3H)-ones as an inhibitor of leishmania folate pathway: In vitro 865
biological evaluation, mechanism studies and molecular docking. 866
Bioorg. Chem. **2019**, *83*, 145–153. 867
- (33) López, S.; Salazar, J.; López, S. E. A Simple One-Pot Synthesis 868
of 2-Substituted Quinazolin-4(3H)-ones from 2-Nitrobenzamidates by 869
Using Sodium Dithionite. *Synthesis* **2013**, *45*, 2043–2050. 870
- (34) Romero, A. H.; Medina, R.; Alcalá, A. M.; García-Marchan, Y.; 871
Núñez-Duran, J.; Leañez, J.; Mijoba, A.; Ciangherotti, C.; Serrano- 872
Martín, X.; López, S. E. Design, synthesis, structure-activity 873
relationship and mechanism of action studies of a series of 4- 874
chloro-1-phthalaziny hydrazones as a potent agent against Leishmania 875
braziliensis. *Eur. J. Med. Chem.* **2017**, *127*, 606–620. 876
- (35) Romero, A. H.; Rodríguez, N.; Oviedo, S. E.; Lopez, H. 877
Antileishmanial activity, mechanism of action study and molecular 878
docking of 1,4-bis(substituted benzalhydrazino)phthalazines. *Arch.* 879
Pharm. **2019**, *352*, No. e1800299. 880
- (36) Alvarez, G.; Martínez, J.; Varela, J.; Birriel, E.; Cruces, E.; 881
Gabay, M.; Leal, S. M.; Escobar, P.; Aguirre-López, B.; Cabrera, N.; 882
Tuena-de Gómez-Puyou, M.; Gómez-Puyou, A.; Pérez-Montfort, R.; 883
Yaluff, G.; Torres, S.; Serna, E.; Vera de Bilbao, N.; González, M.; 884
Cerecetto, H. Development of bis-thiazoles as inhibitors of 885
triosephosphate isomerase from *Trypanosoma cruzi*. Identification 886
of new non-mutagenic agents that are active in vivo. *Eur. J. Med.* 887
Chem. **2015**, *100*, 246–256. 888
- (37) Swiss-ADME, Swiss Institute of Bioinformatics. [http://www.](http://www.swissadme.ch/index.php) 889
[swissadme.ch/index.php](http://www.swissadme.ch/index.php). 890
- (38) Lipinski, C. A.; Lombardo, F.; Dominy, B. W.; Feeney, P. J. 891
Experimental and computational approaches to estimate solubility and 892
permeability in drug discovery and development settings. *Adv. Drug* 893
Deliv. Rev. **2001**, *46*, 3–26. 894
- (39) Daina, A.; Michielin, O.; Zoete, V. SwissADME: a free web tool 895
to evaluate pharmacokinetics, drug-likeness and medicinal chemistry 896
friendliness of small molecules. *Sci. Rep.* **2017**, *7*, 42717. 897
- (40) Baell, J. B.; Holloway, G. A. New Substructure Filters for 898
Removal of Pan Assay Interference Compounds (PAINS) from 899
Screening Libraries and for Their Exclusion in Bioassays. *J. Med.* 900
Chem. **2010**, *53*, 2719–2740. 901
- (41) Cariello, N. F.; Piegorsch, W. W. The Ames test: The two-fold 902
rule revisited. *Mutat. Res.* **1996**, *369*, 23–31. 903
- (42) Gilbert, I. H. Inhibitors of dihydrofolate reductase in 904
Leishmania and trypanosomes. *Biochem. Biophys. Acta* **2002**, *1587*, 905
249–257. 906
- (43) Kumar, A. S.; Kudva, J.; Lahtinen, M.; Peuronen, A.; Sadashiva, 907
R.; Naral, D. Synthesis, characterization, crystal structures and 908
biological screening of 4-amino quinazoline sulfonamide derivatives. 909
J. Mol. Struct. **2019**, *1190*, 29–36. 910
- (44) Suzuki, Y.; Sawada, J.; Hibner, M.; Ishii, A.; Matsuno, R.; Sato, 911
D.; Witulski, B.; Asai, A. Fluorescent anticancer quinazolines as 912

- 913 molecular probes for β -tubulin colchicine site competition assay and
914 visualization of microtubules as intracellular targeting sites. *Dyes*
915 *Pigments* **2017**, *145*, 233–238.
- 916 (45) Motoyama, M.; Doan, J.; Hibner-Kulicka, M.; Otake, A.;
917 Lukarska, R.; Lohier, D. Synthesis and Structure-Photophysics
918 Evaluation of 2-N-Amino-quinazolines: Small Molecule Fluorophores
919 for Solution and Solid State. *Chem.—Asian J.* **2021**, *16*, 2087–2099.
- 920 (46) Held, F. E.; Guryev, J.; Fröhlich, M.; Hampel, A.; Kahnt, R.;
921 Hutterer, D. Facile access to potent antiviral quinazoline heterocycles
922 with fluorescence properties via merging metal-free domino reactions.
923 *Nat. Commun.* **2017**, *8*, 15071.
- 924 (47) Romero, A. H.; Romero, I. E.; Piro, O. E.; Echeverría, G. A.;
925 Gotopo, L.; Moller, M. N.; Rodríguez, G. A.; Cabrera, G. J.; Castro, E.
926 R.; López, S. E.; Cerecetto, H. Photo-Induced Partially Aromatized
927 Intramolecular Charge Transfer. *J. Phys. Chem. B* **2021**, *125*, 9268–
928 9285.
- 929 (48) Miranda, K. M. The chemistry of nitroxyl (HNO) and
930 implications in biology. *Coord. Chem. Rev.* **2005**, *249*, 433–455.
- 931 (49) Romero, A. H.; Rodríguez, N.; López, S. E.; Oviedo, H.
932 Identification of dehydroxy isoquine and isotebuquine as promising
933 antileishmanial agents. *Arch. Pharm.* **2019**, *352*, 1800281.
- 934 (50) Romero, A. H.; Rodríguez, N.; Ramírez, O. G. Optimization of
935 phthalazin-based aryl/heteroarylhydrazones to design new promising
936 antileishmanicidal agents: Synthesis and biological evaluation of 3-
937 aryl-6-piperazin-1,2,4-triazolo[3,4-a]phthalazines. *New J. Chem.* **2020**,
938 *44*, 13807–13814.
- 939 (51) Becke, A. D. A new mixing of Hartree–Fock and local density-
940 functional theories. *J. Chem. Phys.* **1993**, *98*, 1372.
- 941 (52) Petersson, G. A.; Al-Laham, M. A. A complete basis set model
942 chemistry. II. Open-shell systems and the total energies of the first-
943 row atoms. *J. Chem. Phys.* **1991**, *94*, 6081.
- 944 (53) Frisch, M. J.; Trucks, G. W.; Schlegel, H. B.; Scuseria, G. E.;
945 Robb, M. A.; Cheeseman, J. R.; Scalmani, G.; Barone, V.; Mennucci,
946 B.; Petersson, G. A.; et al. *Gaussian 09*, Revision A.1; Gaussian, Inc.:
947 Wallingford, CT, 2009.
- 948 (54) Acosta, M.; Gotopo, L.; Gamboa, N.; Rodrigues, J.; Henriques,
949 G.; Cabrera, G.; Romero, A. H. Antimalarial Activity of Highly
950 Coordinative Fused-Heterocycles Targeting β -Hematin Crystalliza-
951 tion. *ACS Omega* **2022**, *7*, 7499–7514.